J/ψ photoproduction at NLO in NRQCD

M. Butenschön[a*]

[a]II. Institut für Theoretische Physik, Universität Hamburg,
Luruper Chaussee 149, 22761 Hamburg, Germany

We report on the current status of our calculation of the next-to-leading order corrections to both the color singlet and color octet contributions to the J/ψ meson production cross section via direct photoproduction at HERA within the factorization formalism of nonrelativistic quantum chromodynamics (NRQCD).

1. INTRODUCTION

Heavy quarkonia are bound states of a heavy quark and its antiquark. The top quark decays too fast to form a bound state, but there are charmonia and bottomonia. The first time a heavy quarkonium was discovered was in 1974 with the discovery of the J/ψ. This discovery was most important for establishing QCD, in particular its asymptotic freedom. Ever since then heavy quarkonium physics has been an active field for the study of QCD. The calculation of the mass spectrum is a key application for lattice QCD, and the calculation of the production and decay rates has been one of the first applications of perturbative QCD.

Over the years different methods have been devised to calculate these production and decay rates. The classic approach is the so called color singlet model. In that approach the cross section is just assumed to be the cross section for the production/decay of a quarkonium in its physical color singlet, meaning color neutral, state. In case of the J/ψ, this is a charmonium $1^3S_1^{[1]}$ state, where the upper index 1 stands for color singlet. This cross section then has to be multiplied by the quarkonium wave function at the origin or its derivative, respectively. These are treated as numbers extracted from experiment. However, already in the case of P wave quarkonia, there are leftover infrared divergences [1]. This hints at theoretical inconsistencies in this approach.

A newer method is the so called nonrelativistic quantum chromodynamics (NRQCD) [2,3]. This self consistent effective field theory is based on the energy hierarchy

$$Mv^2, Mv \ll \Lambda_{\text{QCD}} \ll M, \qquad (1)$$

which is observed in the quarkonium system. Hereby M is the quarkonium mass and v the relative velocity between the quark and the antiquark. M sets the scale of the pointlike production/decay of the individual quarks, which is accessible in perturbative QCD. The physics of the quarkonium as a whole is however governed by the low energy scales Mv^2, the quarkonium energy, or Mv, the quarkonium momentum scale.

The calculation of the cross section for the production of a heavy quarkonium H within NRQCD is based on the following factorization theorem:

$$\sigma(H) = \sum_n \sigma(c\bar{c}[n]) \cdot \langle \mathcal{O}^H[n] \rangle. \qquad (2)$$

It states that the production cross section factorizes into a short distance part $\sigma(c\bar{c}[n])$, which describes the production of a $c\bar{c}$ pair in a specific Fock state n and is calculated in perturbative QCD, and so called long distance matrix elements (MEs), which express the probability for this $c\bar{c}$ pair to subsequently decay into a physical H via soft gluon radiation. The MEs are in this approach numbers which are extracted by fitting to experimental data. The sum over n is in principal an infinite sum over all possible Fock states, including color octet states. Fortunately, NRQCD predicts each of the MEs $\langle \mathcal{O}^H[n] \rangle$ to scale with a

---

certain power of v, the relative velocity of the c and $\overline{c}$ in the physical H. This relative velocity is a small number which serves as an expansion parameter. In case of J/ψ (with $v^2 \approx 0.2$), NRQCD predicts the leading contribution to come from $n = {}^3S_1^{[1]}$, as $\langle \mathcal{O}^{J/\psi}[{}^3S_1^{[1]}] \rangle$ scales with v^3. This contribution equals the color singlet model prediction. The MEs for $n = {}^1S_0^{[8]}$, ${}^3S_1^{[8]}$ and ${}^3P_{0/1/2}^{[8]}$ all scale with v^7. These contributions are called the relativistic corrections or *the* color octet contributions. All other MEs scale with higher powers of v.

In this framework, the leftover infrared divergences of the P wave quarkonia are canceled by NRQCD radiative corrections to the MEs of S states, as will be described in section 4.2.

The great breakthrough for NRQCD had been that it was able to explain the cross section for J/ψ hadroproduction at the Tevatron [4], which is orders of magnitude larger than the color singlet model prediction, see figure 1. However, in order to establish NRQCD as the correct theory for heavy quarkonium production, it is indispensable to show the significance of the color octet contributions in other high energy experiments as well. In case of direct photoproduction at HERA, the color singlet model prediction at NLO in α_s describes the data very well [5]. On the other hand, a Born level NRQCD calculation including intermediate color octet states and using values for the MEs obtained from fits to the Tevatron data, predicts a rise in the cross section at high z which is not observed [6,7], see figure 2. This situation does not support the universality of the MEs, a key element of the NRQCD factorization. In order to clarify the situation it is therefore necessary to perform the NRQCD calculation also at NLO in α_s. That is the aim of our current work.

The NLO corrections for color singlet states are known for the direct photoproduction [5] and since recently also for the hadroproduction [8,9]. As for NLO corrections to inclusive quarkonium production including color octet states, there has so far only been one complete calculation, the J/ψ production rate in two-photon collisions [10]. However, that calculation was not complicated by virtual corrections to intermediate p states.
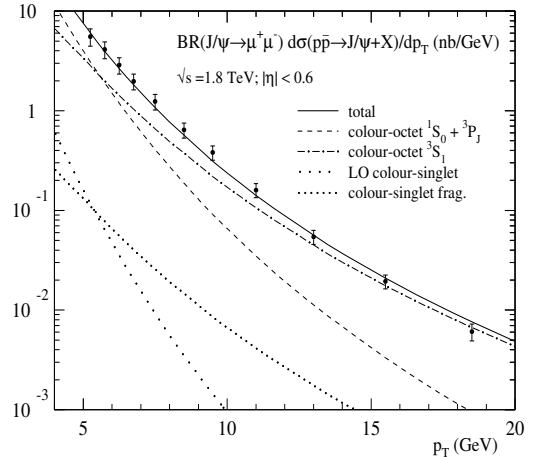

Figure 1. Different leading order contributions to the p_T distribution of inclusive J/ψ hadroproduction at the Tevatron. This figure is taken from [11].
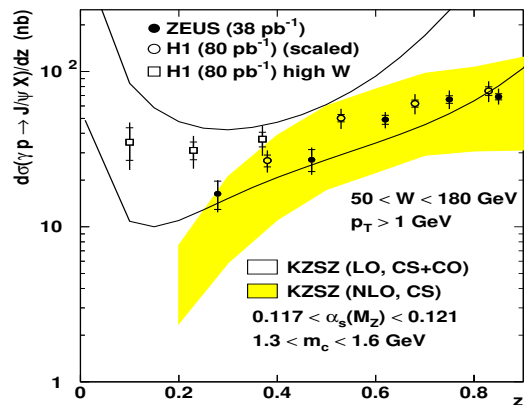

Figure 2. The z distribution of inclusive J/ψ photoproduction at HERA. This figure is taken from [12]. The open bands represents the leading order color singlet plus color octet contributions in direct and resolved photoproduction. The resolved contribution is dominant in the low z region. The solid band represents the NLO color singlet contribution for direct photoproduction. The plotted theoretical uncertainties are due to uncertainties in the size of the charm quark mass and the color octet MEs.

2. OVERVIEW: OUR CALCULATION

In direct photoproduction an on-shell bremsstrahlung photon, which is radiated off the incoming electron, interacts with a parton i stemming from the incoming proton. We calculate the hadronic cross section by folding the partonic cross section with the proton parton distribution functions (PDFs) and the Weizsäcker-Williams distribution [13]. The partonic cross section is then calculated according to the NRQCD factorization theorem (2), so that

$$
\begin{aligned}
&d\sigma(e^- p \to J/\psi + X) \\
&= \int dx f_{\gamma/e}(x) \sum_i \int dy f_{i/p}(y) \\
&\quad \times \sum_n d\sigma(\gamma i \to c\bar{c}[n] + X) \cdot \langle \mathcal{O}^{J/\psi}[n] \rangle. \quad (3)
\end{aligned}
$$

The cross section for the production of a $c\bar{c}$ pair in a Fock state n, $d\sigma(\gamma i \to c\bar{c}[n])$, is calculated from amplitudes which we get by applying certain projectors onto the usual QCD amplitudes for open $c\bar{c}$ production. In the notation of [14]:

$$
\mathcal{A}_{^1S_0^{[8]}} = \text{Tr}\left[\mathcal{C}_8 \Pi_0 \mathcal{A} \right]|_{q=0}, \quad (4)
$$

$$
\mathcal{A}_{^3S_1^{[1/8]}} = \mathcal{E}_\alpha \text{Tr}\left[\mathcal{C}_{1/8} \Pi_1^\alpha \mathcal{A} \right]|_{q=0}, \quad (5)
$$

$$
\mathcal{A}_{^3P_J^{[8]}} = \mathcal{E}_{\alpha\beta}^J \frac{\partial}{\partial q_\beta} \text{Tr}\left[\mathcal{C}_8 \Pi_1^\alpha \mathcal{A} \right]|_{q=0}. \quad (6)
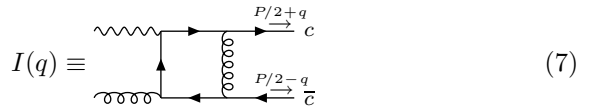$$

$\mathcal{A}$ are the QCD amplitudes with amputated charm spinors. $\Pi_{0/1}$ are spin projectors onto the spin singlet and spin triplet states. $\mathcal{C}_{1/8}$ are color projectors onto the color singlet and color octet states. $\mathcal{E}_\alpha$ and $\mathcal{E}_{\alpha\beta}$ are polarization vectors of the $c\bar{c}$ state. In case of intermediate S states, we have to set the relative momentum $2q$ between the two external charm quarks to zero, and in the case of intermediate P states, we have to evaluate the derivative with respect to q at the point $q = 0$.

2.1. No Coulomb Divergences

In the case of the virtual correction diagrams we also have to perform the loop integration. In previous calculations, e.g. [5,9,10,14,15], the loop integration was performed, before the projectors were applied. The results then contain Coulomb singularities stemming from loop diagrams with a gluon exchange between the two external quark lines. These Coulomb singularities are regularized by rewriting the relative momentum $2q$ in terms of the relative velocity v, which is kept as a small parameter. In those papers the authors either absorb them into the quarkonium wave functions of the color singlet model [5,9,15], or they claim that they are canceled by radiative corrections due to longitudinal gluon exchange in the virtual corrections to the MEs [10,14].

Our approach is different. We first apply the projectors and then perform the loop integration. Then our results are free of Coulomb divergences. Consider for example the following diagram:

$$
I(q) \equiv
$$

If you first evaluate the integral with arbitrary q and then apply the projectors, which eventually means setting $q \to 0$, the result will have the form

$$
\lim_{q \to 0} I(q) = \frac{A}{q^2} + \frac{B}{\epsilon} + C, \quad (8)
$$

where B/ϵ is the infrared divergency and A/q^2 the Coulomb divergent term. On the other side, in our method, we directly evaluate the integral at $q = 0$ and our result is

$$
I(0) = \frac{B}{\epsilon} + C, \quad (9)
$$

with the same B and C as in (8), but without the Coulomb divergent term. It is a well known feature that Coulomb singularities are not apparent in dimensional regularization [16]. Besides not having to deal with Coulomb singularities, our approach has the advantage that after setting q to zero, we have one mass scale less in the loop integration. However now our loop integrals consist of propagators with linearly dependent propagator momenta. This point will be further addressed in section 3.

We have also calculated the radiative corrections to the MEs in dimensional regularization, and the results are free of Coulomb singularities as well. Moreover the contributions from Coulomb gluon exchange are exactly zero. For more details, see section 4.2.

2.2. Our Treatment of γ_5

The projector Π_0 in (4) for the spin singlet $c\bar{c}[^1S_0^{[8]}]$ state contains a γ_5. When applying this projector on our amplitudes we have to evaluate a spin trace over one γ_5 and up to eight other gamma matrices. Therefore we have to implement the 't Hooft-Veltman or also called the Breitenlohner-Maison scheme, which was first proposed in [17] and elaborated in [18]. The aspects important for this calculation are comprehensively summarized in [19].

We replace each γ_5 by

$$\gamma_5 = \frac{i}{4!}\epsilon_{\mu\nu\rho\sigma}\gamma^\mu\gamma^\nu\gamma^\rho\gamma^\sigma. \tag{10}$$

Here, the gamma matrices on the right hand side are $n = 4 - 2\epsilon$ dimensional, but the Levi-Civita tensor ϵ is a 4 dimensional object. The n dimensional dirac trace in (4) can now be performed. The squared amplitude for producing a $c\bar{c}[^1S_0^{[8]}]$ state then still contains exactly two ϵ tensors, which are further evaluated using the identity

$$\epsilon^{\alpha_1\alpha_2\alpha_3\alpha_4}\epsilon^{\beta_1\beta_2\beta_3\beta_4} = -\det\left(\tilde{g}^{\alpha_i\beta_j}\right). \tag{11}$$

Hereby the $\tilde{g}^{\alpha_i\beta_j}$ are 4 dimensional metric tensors, which are treated according to

$$\tilde{g}_{\mu\nu}g^{\nu\rho} = \tilde{g}_\mu^\rho, \quad \tilde{g}_{\mu\nu}p^\nu = \tilde{p}_\mu, \quad \tilde{g}_{\mu\nu}\tilde{g}^{\mu\nu} = 4, \tag{12}$$

where $g^{\nu\rho}$ and p^ν are n dimensional and $\tilde{p}_\mu$ is 4 dimensional. This method does not include any counterterms.

2.3. The Implementation

We have implemented our calculation in the following way. We use FeynArts [20] to generate the diagrams needed for all subprocesses. After that we use a Mathematica [21] script to separate the color structure from the rest of the amplitudes, apply the color projectors for color singlet and color octet states $c\bar{c}[n]$ and evaluate all color factors with FeynCalc [22]. The non-color part of the amplitudes is then further treated by a FORM [23] script, which applies the spin part of the projectors onto the various $c\bar{c}[n]$ states, squares the amplitudes, performs the polarization sums and fermion traces and recombines the results with the color factors.

In the case of the virtual corrections, we still have to perform the loop integrations. This part is implemented in a combination of different FORM scripts. We have implemented two different methods. Details will follow in section 3. In the first method we first apply our own tensor reduction formulas, thereby reducing the integrals to scalar integrals. After that we reduce the integrals further to a set of 14 master integrals by using reduction formulas which we derive from integration by parts relations with the help of the program AIR [24] which makes use of the Laporta algorithm [25]. In the second implementation we do not perform a tensor reduction, but instead express all scalar products in the numerators as a sum of propagators, which is always possible. After a cancellation we then end up with scalar integrals with negative propagator powers. These scalar integrals are now directly reduced to the master integrals by using the reduction formulas derived with AIR. However, this second method cannot be used for the production of the spin singlet state $c\bar{c}[^1S_0^{[8]}]$. The reason is that here, as explained in section 2.2, we will have 4 dimensional scalar products in the numerators besides the usual n dimensional ones. In case of external momenta, there is no difference, but a 4 dimensional scalar product $\tilde{Q}^2$ of a loop momentum does not necessarily equal its n dimensional counterpart Q^2. Therefore we cannot cancel a $\tilde{Q}^2$ in the numerator against a Q^2 propagator, so we cannot express tensor integrals with $\tilde{Q}^2$ numerators only in terms of scalar integrals.

The results coming out of these FORM programs are of the order of hundreds of megabytes in size for each subprocess. In order to process the expressions further we devised a Mathematica script which simplifies the results by using the usual identities relating the different Mandelstam variables. This simplification process is the most time consuming part of the implementation, but we gain a reduction of the expressions in size by up to a factor 2000. After that the expressions are of manageable size, and we could analytically show that, first, the results of the two methods for doing the loop integration are equal and, second, all divergences, the ultraviolet as well as the in-

frared ones, vanish in the sum of all contributions. This cancellation of divergences is described in more detail in section 4.

The remaining step is the numerical evaluation in a FORTRAN program, which we are currently still working on. Thereby we have implemented the phase space slicing method of [26].

3. VIRTUAL CORRECTIONS

In this section we go into more details with the procedure we used to reduce the loop integrals occurring in the virtual corrections to a set of master integrals.

3.1. The Tensor Reduction

A typical Feynman diagram appearing in our calculation looks like this:
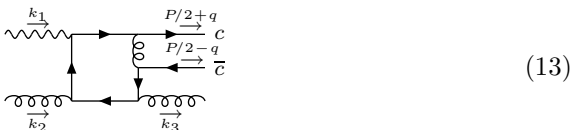
As addressed in section 2, projecting onto the specific $c\bar{c}[n]$ states leads to tensor integrals with linearly dependent propagator momenta, and in the case of P states also to double propagator powers due to the derivative with respect to the relative momentum $2q$ between the charm and the anticharm. A sample integral is

$$\int \frac{d^D Q \, Q^\mu Q^\nu}{Q^2 \left[(Q+\frac{P}{2})^2 - m^2\right]\left[(Q-\frac{P}{2})^2 - m^2\right]^2}, \quad (14)$$

where m is the charm quark mass, Q the loop momentum, and P the J/ψ momentum. A direct application of the Passarino-Veltman [27] reduction formulas is of course not possible, as we would have to call for example the integral (14) a D function, like $D^{\mu\nu}(P/2, -P/2, -P/2, 0, m, m, m)$. This would lead to zero Gram determinants, by which we would have to divide in the course of the reduction procedure. As a side remark, we mention that this is a different case than the one studied in [28]. In that paper the problem of numerical instabilities due to small Gram determinants is addressed and not the case of zero Gram determinants.

In our tensor reduction procedure we classify the integrals not according to the number of prop-

agators, but according to the number of independent momenta appearing in them. Therefore we call for example the integral (14) a B function, for which we write the tensor decomposition as

$$B^{\mu\nu} = g^{\mu\nu} B_{1,0} + \frac{1}{4} P^\mu P^\nu B_{0,2}, \quad (15)$$

where $B_{1,0}$ and $B_{0,2}$ are tensor coefficients, which are expressed in terms of scalar integrals.

We have derived general tensor reduction formulas which can reduce tensor integrals with an arbitrary number of Lorentz indicies in the numerator and up to four linearly independent momenta in the propagators. Furthermore the momentum of one propagator may depend linearly on the momenta of the other propagators and on top of this we allow for one propagator to have a double power. These formulas are general enough to reduce all tensor integrals appearing in our calculation to scalar ones.

3.2. Integration by Parts

The method of integration by parts, which was originally proposed in [29], is based on the following two properties of any dimensionally regularized Feynman integral f with loop momenta Q_i and external momenta p_i:

$$0 = \frac{\partial}{\partial Q^\mu} Q_i^\mu f(Q_1, \ldots, Q_n, p_1, \ldots, p_m)$$
$$0 = \frac{\partial}{\partial Q^\mu} p_i^\mu f(Q_1, \ldots, Q_n, p_1, \ldots, p_m) \quad (16)$$

A *topology* is a class of Feynman integrals which only differ in the powers of the propagators. If we apply (16) to a diagram with general propagator powers λ_i, we obtain relations between different members of the corresponding topology. Particular linear combinations of these relations can then express integrals in terms of others with lower (or less negative) propagator powers. Thus a reduction to a set of master integrals can be achieved.

Usually, integration by parts is used in multi loop calculations, as one loop integrals which appear in normal QCD calculations are already master integrals. In the case of our integrals with linearly dependent propagator momenta and double propagator powers, however, this method works very effectively. All scalar integrals can be

expressed as a member of one of the following four topologies:

$$T_1 = \cdots \quad T_2 = \cdots \quad (17)$$
$$T_3 = \quad T_4 =$$

Here, the solid lines are the massive c quark lines, and the dashed lines are massless lines. The propagator powers λ_i can be 0, 1 or 2.

The reduction process leads to just 14 master integrals: 4 boxes, 5 triangles, 4 bubbles and 1 tadpole. All of these are standard integrals, of which we know the complete analytical result in dimensional regularization.

One feature of the integration by parts procedure is that after the reduction we can not distinguish between ultraviolet and infrared singularities any more. This can be seen for example from the fact that the reduced expressions contain terms like $B_0(\ldots)/\epsilon$, where B_0 is a usual 2 point function. Here, the resulting $1/\epsilon^2$ singularity must of course be infrared, but we can not say anything about the nature of the resulting $1/\epsilon$ singularities. In order to distinguish between ultraviolet and infrared singularities we therefore extract the ultraviolet singularities from the scalar integrals before application of the integration by parts reduction formulas.

4. THE DIVERGENCY STRUCTURE

The loop integrals of the virtual correction diagrams lead to both ultraviolet and infrared divergences. The ultraviolet divergences are canceled by the renormalization of the strong coupling constant and the charm quark mass and by the wave function renormalizations of the external particles.

As for the infrared divergences, there are contributions from different sources which all cancel in the end. An overview over these cancellations is visualized in figure 3. The real correction contributions contain infrared divergences both in the soft and the collinear limits. These are to a large extent canceled by the virtual correction contributions, which contain infrared singularities coming from the loop diagrams and the

wave function renormalizations. The structure of the soft singularities will be described in more detail in section 4.1. The infrared singularity arising from an outgoing parton which is collinear to the incoming parton stemming from the proton is absorbed into the corresponding PDF of the proton. The collinear singularity arising when an outgoing parton is collinear to the incoming photon is actually only canceled when we also include the NLO corrections of the resolved photoproduction process, because that collinear singularity can then be absorbed into the photon PDF. We make use of this absorption, although we do in this calculation actually not yet consider the complete resolved photoproduction cross section. A last source of infrared singularities are the α_s corrections to the $\langle \mathcal{O}^{J/\psi}[^3S_1^{[1/8]}] \rangle$ long distance matrix elements, as will be described in more detail in section 4.2.

4.1. Soft Divergences

Soft divergences occur when a soft gluon is emitted from an external QCD parton line. Consider the following general real correction amplitude

$$(18)$$

where the dashed lines can be photons or QCD partons (gluons or quarks). If the gluon with momentum k_4 is soft, (18) factorizes according to

$$|k_4 \text{ soft}\rangle = g_s \left(\frac{q \cdot \epsilon^*(k_4)}{(\frac{P}{2} + q) \cdot k_4} \mathbf{T_c} - \frac{q \cdot \epsilon^*(k_4)}{(\frac{P}{2} - q) \cdot k_4} \mathbf{T_{\bar{c}}} \right.$$
$$\left. + \sum_{i=1}^{3} \frac{k_i \cdot \epsilon^*(k_4)}{k_i \cdot k_4} \mathbf{T_i} \right) |\text{Born}\rangle. \quad (19)$$

Here, the sum over i is meant to run only over those external particles which are QCD partons, so in direct photoproduction with particle 1 being a photon, it runs from 2 to 3. $|\text{Born}\rangle$ denotes the born amplitude which we get when removing the gluon with momentum k_4. The color operators $\mathbf{T_x}$ for each particle x are the ones defined in [30]: They act on $|\text{Born}\rangle$ by the insertion of a
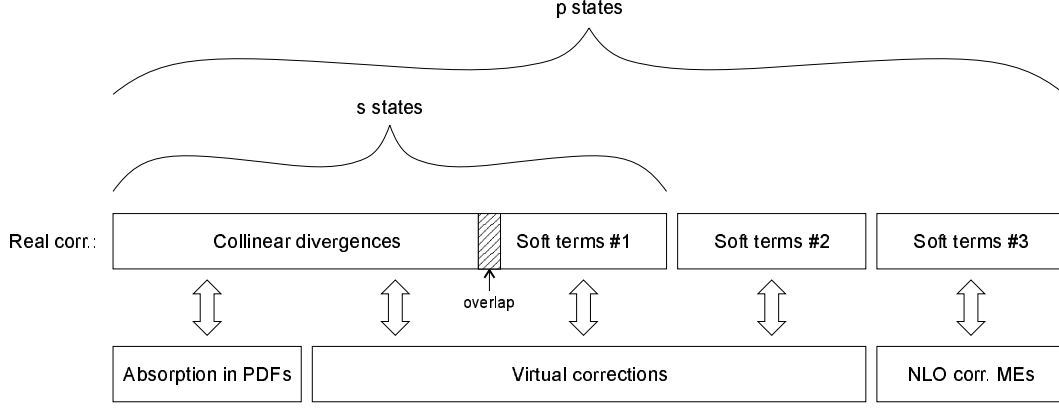
Figure 3. Overview over the infrared singularity structure and its cancellations

color matrix T_c or a structure constant f_{abc} at the position of the corresponding particle in the amplitude. Furthermore, in the calculation of the soft limits we use the axial gauge, where

$$\sum \epsilon^\mu(k_4)\epsilon^{*\nu}(k_4)$$
$$= -g^{\mu\nu} + \frac{P^\mu k_4^\nu + k_4^\mu P^\nu}{P \cdot k_4} - \frac{P^2 k_4^\mu k_4^\nu}{(P \cdot k_4)^2}, \quad (20)$$

so that $P \cdot \epsilon(k_4) = 0$.

Application of the projectors (4) – (6) and squaring of the amplitudes leads to the following expressions for the squared matrix elements of the real corrections in the limit $k_4 \to 0$:

$$\left\langle {}^1S_0^{[8]}, k_4 \text{ soft}\middle| {}^1S_0^{[8]}, k_4 \text{ soft}\right\rangle = S_1({}^1S_0^{[8]}), \quad (21)$$

$$\left\langle {}^3S_1^{[1/8]}, k_4 \text{ soft}\middle| {}^3S_1^{[1/8]}, k_4 \text{ soft}\right\rangle = S_1({}^3S_1^{[1/8]}), (22)$$

$$\left\langle {}^3P_J^{[8]}, k_4 \text{ soft}\middle| {}^3P_J^{[8]}, k_4 \text{ soft}\right\rangle = S_1({}^3P_J^{[8]})$$
$$+ S_2^J + S_3^J, \quad (23)$$

where we have abbreviated the soft terms type 1,

$$S_1(n) = g_s^2 \sum_{i,j=1}^3 \frac{k_i \cdot \epsilon(k_4) \; k_j \cdot \epsilon^*(k_4)}{k_i \cdot k_4 \; k_j \cdot k_4}$$
$$\times \left\langle n, \text{Born}\middle| \mathbf{T_i} \, \mathbf{T_j} \middle| n, \text{Born}\right\rangle, \quad (24)$$

which appear both in intermediate S and P states, and the soft terms of type 2 and 3,

$$S_2^J = 4g_s^2 \sum_{i=1}^3 \frac{k_i \cdot \epsilon(k_4) \; \epsilon^{*\beta}(k_4)}{k_i \cdot k_4 \; P \cdot k_4} \left\langle {}^3P_J^{[8]}, \text{Born}\middle| \mathbf{T_i} \right.$$
$$\times (\mathbf{T_c} - \mathbf{T_{\overline{c}}}) \, \mathcal{E}_{\alpha\beta}^J \text{Tr}\left[\mathcal{C}_8 \Pi_1^\alpha \middle| \text{Born}\right\rangle\right]\Big|_{q=0}, \quad (25)$$

$$S_3^J = 4g_s^2 \frac{\epsilon^{\beta^*}(k_4) \; \epsilon^{*\beta}(k_4)}{(P \cdot k_4)^2} \mathcal{E}_{\alpha^*\beta^*}^{*J} \mathcal{E}_{\alpha\beta}^J$$
$$\times \text{Tr}\left[\left\langle \text{Born}\middle| \Pi_1^{*\alpha^*} \mathcal{C}_8\right]\Big|_{q=0} (\mathbf{T_c} - \mathbf{T_{\overline{c}}})\right.$$
$$\times (\mathbf{T_c} - \mathbf{T_{\overline{c}}}) \text{Tr}\left[\mathcal{C}_8 \Pi_1^\alpha \middle| \text{Born}\right\rangle\right]\Big|_{q=0}, \quad (26)$$

which appear additionally in the ${}^3P_J$ states, see figure 3.

The divergences stemming from the soft terms of type 1 and 2 are canceled by the virtual corrections. Now let us have a closer look at the soft terms of type 3: Summing over the polarizations of the external particles and integrating k_4 over the soft region of phase space results in

$$\int_{\text{soft}} dPS_{k_4} \, \overline{S_3^J} = 4g_s^2 \overline{\left\langle {}^3S_1^{[8]}, \text{Born}\middle| (\mathbf{T_c} - \mathbf{T_{\overline{c}}}) \right.}$$
$$\times \overline{(\mathbf{T_c} - \mathbf{T_{\overline{c}}}) \middle| {}^3S_1^{[8]}, \text{Born}\right\rangle}$$
$$\times \frac{2 - 2\epsilon}{(3 - 2\epsilon)^2} N_J \int_{\text{soft}} \frac{dPS_{k_4}}{(P \cdot k_4)^2}. \quad (27)$$

Here, N_J is the number of polarizations of a spin-J state in $n = 4 - 2\epsilon$ dimensions. Moreover, at least in the processes under consideration, we have:

$$
\begin{aligned}
&\overline{\langle {}^3S_1^{[8]},\, \text{Born}|\,(\mathbf{T_c} - \mathbf{T_{\overline{c}}})(\mathbf{T_c} - \mathbf{T_{\overline{c}}})\,|{}^3S_1^{[8]},\, \text{Born}\rangle} \\
&= \frac{C_A^2 - 4}{C_A}\,\overline{\langle {}^3S_1^{[8]},\, \text{Born}|{}^3S_1^{[8]},\, \text{Born}\rangle} \\
&\quad + 4C_F\,\overline{\langle {}^3S_1^{[1]},\, \text{Born}|{}^3S_1^{[1]},\, \text{Born}\rangle},
\end{aligned} \tag{28}
$$

with $C_A = N_C$, $C_F = (N_C^2 - 1)/(2N_C)$ and N_C being 3 in QCD. So we see that the infrared divergences emerging from the soft terms of type 3 are proportional to the Born squared matrix elements of the ${}^3S_1$ states.

4.2. α_s Corrections to $\langle \mathcal{O}^{J/\psi}[{}^3S_1^{[1/8]}]\rangle$

Within the framework of NRQCD, the long distance matrix elements $\langle \mathcal{O}^{J/\psi}[n]\rangle$ are vacuum expectation values of four-fermion operators:

$$
\begin{aligned}
\langle \mathcal{O}^{J/\psi}[n]\rangle &= \langle c\overline{c}[n]\big|J/\psi + X\rangle\langle J/\psi + X\big|c\overline{c}[n]\rangle \\
&= \langle 0\big| \underbrace{\chi^\dagger \mathcal{K}_{i,j,a}^n \psi\, \mathcal{P}^{J/\psi}\, \psi^\dagger \mathcal{K}_{i,j,a}^n \chi}_{\text{4-fermion operator } \mathcal{O}^{J/\psi}[n]} \big|0\rangle,
\end{aligned} \tag{29}
$$

with

$$
\mathcal{P}^{J/\psi} = \big|J/\psi + X\rangle\langle J/\psi + X\big|, \tag{30}
$$

where X stands for all other particles which are produced during the $c\overline{c}[n] \to J/\psi$ transition, e.g. soft gluons. ψ is the Pauli field operator annihilating a charm quark and χ the Pauli field creating an anticharm quark. The factors $\mathcal{K}_{i,j,a}^n$ consist of Pauli matrices σ_i, color matrices T_a and in case of p states also of field derivation operators. Their complete forms can be found in [3].

Following the approach of [3,14], we interpret (29) as NRQCD Feynman amplitudes for $c\overline{c}$ scattering. At leading order we have:

$$
\langle \mathcal{O}^{J/\psi}[{}^3S_1^{[8]}]\rangle_{\text{Born}} =
$$

$$
= C\, \xi^\dagger(\mathbf{p}')\sigma_i T_a \eta(-\mathbf{p}')\, \eta^\dagger(-\mathbf{p})\sigma_i T_a \xi(\mathbf{p}), \tag{31}
$$

$$
\sum_{J=0}^{2}\langle \mathcal{O}^{J/\psi}[{}^3P_J^{[8]}]\rangle_{\text{Born}} =
$$

$$
\begin{aligned}
= {}&C\, \mathbf{p}\cdot\mathbf{p}'\, \xi^\dagger(\mathbf{p}')\sigma_i T_a \eta(-\mathbf{p}') \\
&\times \eta^\dagger(-\mathbf{p})\sigma_i T_a \xi(\mathbf{p}),
\end{aligned} \tag{32}
$$

where ξ is the Pauli spinor of the incoming c quark and η the Pauli spinor of the outgoing $\overline{c}$ quark. C is an overall constant. The expressions for the corresponding color singlet MEs are the same as (31) and (32), but without the color matrices T_a.

Let us now consider α_s corrections to these MEs. The Feynman diagrams throughout this subsection are pure NRQCD diagrams. Because of the nonrelativistic structure of the theory, it is most convenient to use the Coulomb gauge for the gluon propagator. Consider the following diagram with transverse gluon exchange:

$$
\begin{aligned}
= {}&C\, \xi^\dagger(\mathbf{p}')\sigma_i T_b T_a \eta(-\mathbf{p}') \\
&\times \eta^\dagger(-\mathbf{p})\sigma_i T_a T_b \xi(\mathbf{p}) \cdot I,
\end{aligned} \tag{33}
$$

where

$$
\begin{aligned}
I = {}&-\frac{g_s^2}{m^2}\int \frac{d^n k}{(2\pi)^4}\, p_i(p_j' - k_j)\frac{i(\delta_{ij} - k_i k_j/|\mathbf{k}|^2)}{k^2 + i\epsilon} \\
&\times \frac{i}{\frac{\mathbf{p}^2}{2m} - k_0 - \frac{(\mathbf{p} - \mathbf{k})^2}{2m} + i\epsilon} \\
&\times \frac{i}{\frac{\mathbf{p}'^2}{2m} - k_0 - \frac{(\mathbf{p}' - \mathbf{k})^2}{2m} + i\epsilon}.
\end{aligned} \tag{34}
$$

Here we have used NRQCD Feynman rules for the quark gluon vertex and the heavy quark propagator and the on shell conditions $p_0 = |\mathbf{p}|/2m$ and $p_0' = |\mathbf{p}'|/2m$ with m the charm mass. A crucial feature of NRQCD calculations is that the heavy quark propagator has to be expanded in $1/m$ before integration [31]. Otherwise one would get a wrong result, because NRQCD is valid only in the region $\mathbf{k}^2, \mathbf{p}^2, \mathbf{p}'^2 \ll m^2$. So keeping only the leading term in $1/m$ and performing a contour integration over k_0 yields:

$$
\begin{aligned}
I &= \frac{g_s^2}{m^2}\int \frac{d^{n-1}k}{(2\pi)^3}\left(\mathbf{p}\cdot\mathbf{p}' - \frac{\mathbf{p}\cdot\mathbf{k}\,\mathbf{p}'\cdot\mathbf{k}}{|\mathbf{k}|^2}\right)\frac{1}{2|\mathbf{k}|^3} \\
&= \frac{g_s^2}{12\pi^2 m^2}\mathbf{p}\cdot\mathbf{p}'\left(\frac{1}{\epsilon_{\text{UV}}} - \frac{1}{\epsilon_{\text{IR}}}\right).
\end{aligned} \tag{35}
$$

Besides (33) there are three other, similar diagrams contributing to the α_s corrections. The sum of all four of them is:

$$\langle\mathcal{O}^{J/\psi}[^3S_1^{[8]}]\rangle_{\alpha_s} = 2IC\Big[\xi^\dagger(\mathbf{p}')\sigma_i T_b T_a \eta(-\mathbf{p}')$$
$$\times\eta^\dagger(-\mathbf{p})\sigma_i T_a T_b \xi(\mathbf{p}) + \xi^\dagger(\mathbf{p}')\sigma_i T_a T_b \eta(-\mathbf{p}')$$
$$\times\eta^\dagger(-\mathbf{p})\sigma_i T_a T_b \xi(\mathbf{p})\Big]$$
$$= \frac{g_s^2}{6\pi^2 m^2}\sum_J\left[\left(\frac{C_A}{2}-\frac{2}{C_A}\right)\langle\mathcal{O}^{J/\psi}[^3P_J^{[8]}]\rangle_{\mathrm{Born}}\right.$$
$$\left.+\frac{C_F}{C_A}\langle\mathcal{O}^{J/\psi}[^3P_J^{[1]}]\rangle_{\mathrm{Born}}\right]\left(\frac{1}{\epsilon_{\mathrm{UV}}}-\frac{1}{\epsilon_{\mathrm{IR}}}\right).\text{(36)}$$

Similarly we have

$$\langle\mathcal{O}^{J/\psi}[^3S_1^{[1]}]\rangle_{\alpha_s} = \frac{g_s^2}{3\pi^2 m^2}\sum_J\langle\mathcal{O}^{J/\psi}[^3P_J^{[8]}]\rangle_{\mathrm{Born}}$$
$$\times\left(\frac{1}{\epsilon_{\mathrm{UV}}}-\frac{1}{\epsilon_{\mathrm{IR}}}\right).\tag{37}$$

The $1/\epsilon_{\mathrm{UV}}$ divergences are canceled by renormalization of the MEs. The $1/\epsilon_{\mathrm{IR}}$ divergences then cancel the soft divergences of type 3 of the P wave real corrections.

All diagrams with Coulomb gluon exchange are exactly zero. However, the authors of [10,14] claim that diagrams like

$$\tag{38}$$

contain Coulomb singularities which cancel the Coulomb singularities appearing in their short distance cross sections. But that is due to the fact that they have performed the loop integration in (38) before expanding in $1/m$.

5. SUMMARY

Nonrelativistic QCD provides a rigorous factorization theorem for the production of heavy quarkonia. A key feature is the inclusion of intermediate color octet, meaning color charged, states. These color octet states are needed for the description of the p_T distribution of the J/ψ hadroproduction cross section at the Tevatron. In case of the J/ψ photoproduction at HERA, however, the NRQCD Born calculation using values for the MEs obtained from the Tevatron data suggests the sum of color singlet and color octet contributions might overshoot the data in the high z region. In order to clarify the situation, we therefore do a NRQCD calculation of the direct J/ψ photoproduction at NLO in α_s.

We have found a way to calculate the virtual correction diagrams without having to deal with Coulomb singularities like in previous calculations in the field of heavy quarkonium production. We have implemented two methods for the reduction of the appearing loop integrals to master integrals and could analytically show that the results of these two methods are equal. We could analytically proof the cancellation of all divergences appearing in our calculation, for the ultraviolet ones and the infrared ones separately. At this stage of the work, we can not present final results yet, as we are still working on the numerical evaluation, but we are about to finish the calculation soon.

REFERENCES

1. R. Barbieri, R. Gatto and E. Remiddi, Phys. Lett. B **61**, 465 (1976).
2. W. E. Caswell and G. P. Lepage, Phys. Lett. B **167**, 437 (1986).
3. G. T. Bodwin, E. Braaten and G. P. Lepage, Phys. Rev. D **51**, 1125 (1995) [Erratum-ibid. D **55**, 5853 (1997)].
4. P. L. Cho and A. K. Leibovich, Phys. Rev. D **53**, 150 (1996); P. L. Cho and A. K. Leibovich, Phys. Rev. D **53**, 6203 (1996).
5. M. Krämer, Nucl. Phys. B **459**, 3 (1996).
6. M. Cacciari and M. Krämer, Phys. Rev. Lett. **76**, 4128 (1996).
7. P. Ko, J. Lee and H. S. Song, Phys. Rev. D **54**, 4312 (1996) [Erratum-ibid. D **60**, 119902 (1999)].
8. J. Campbell, F. Maltoni and F. Tramontano, Phys. Rev. Lett. **98**, 252002 (2007).
9. B. Gong and J. X. Wang, Phys. Rev. Lett. **100**, 232001 (2008).
10. M. Klasen, B. A. Kniehl, L. N. Mihaila and M. Steinhauser, Nucl. Phys. B **713**, 487

(2005).

11. M. Krämer, Prog. Part. Nucl. Phys. **47**, 141 (2001).

12. N. Brambilla *et al.* [Quarkonium Working Group], arXiv:hep-ph/0412158 (2005).

13. E. J. Williams, Proc. R. Soc. London A **139**, 163 (1933); C. F. v. Weizsäcker, Z. Phys. **88**, 612 (1934).

14. A. Petrelli, M. Cacciari, M. Greco, F. Maltoni and M. L. Mangano, Nucl. Phys. B **514**, 245 (1998).

15. Y. J. Zhang, Y. J. Gao and K. T. Chao, Phys. Rev. Lett. **96**, 092001 (2006); Y. J. Zhang and K. T. Chao, Phys. Rev. Lett. **98**, 092003 (2007).

16. A. Pineda and J. Soto, Phys. Rev. D **58**, 114011 (1998).

17. G. 't Hooft and M. J. G. Veltman, Nucl. Phys. B **44**, 189 (1972).

18. P. Breitenlohner and D. Maison, Commun. Math. Phys. **52**, 11 (1977).

19. J. G. Körner, G. Schuler, G. Kramer and B. Lampe, Phys. Lett. B **164**, 136 (1985).

20. T. Hahn, Comput. Phys. Commun. **140**, 418 (2001).

21. Wolfram Research, Inc., Mathematica, Version 5.2, Champaign, IL (2005).

22. R. Mertig, M. Böhm and A. Denner, Comput. Phys. Commun. **64**, 345 (1991).

23. J. A. M. Vermaseren, Report No. NIKHEF-00-032, arXiv:math-ph/0010025 (2000).

24. C. Anastasiou and A. Lazopoulos, JHEP **0407**, 046 (2004).

25. S. Laporta, Int. J. Mod. Phys. A **15**, 5087 (2000).

26. B. W. Harris and J. F. Owens, Phys. Rev. D **65**, 094032 (2002).

27. G. Passarino and M. J. G. Veltman, Nucl. Phys. B **160**, 151 (1979).

28. A. Denner and S. Dittmaier, Nucl. Phys. B **734**, 62 (2006).

29. K. G. Chetyrkin and F. V. Tkachov, Nucl. Phys. B **192**, 159 (1981).

30. S. Catani and M. H. Seymour, Nucl. Phys. B **485**, 291 (1997) [Erratum-ibid. B **510**, 503 (1998)]; S. Catani, S. Dittmaier, M. H. Seymour and Z. Trocsanyi, Nucl. Phys. B **627**, 189 (2002).

31. A. V. Manohar, Phys. Rev. D **56**, 230 (1997).